A Redox-Switcheroo: Oxidizing a series of olefin metathesis catalysts outfitted with ferrocene-containing *N*-heterocyclic carbene ligands was found to reduce their activities in ring-closing metathesis reactions; subsequent reduction restored the catalytic activities, even over multiple cycles (see figure).

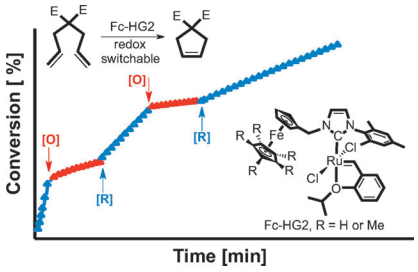

Jolting electrons…
…out of catalysts bearing redox-active ferrocene groups reduces their activities in ring-closing metathesis reactions; subsequent reduction restores catalytic performance. For more details see the Full Paper by C. W. Bielawski et al. on page ▮▮. The authors are indebted to Dr. Angel Syrett for her kind assistance with the graphics.

DOI: 10.1002/chem.201301247

Redox-Switchable Ring-Closing Metathesis: Catalyst Design, Synthesis, and Study

Kuppuswamy Arumugam,[a] C. Daniel Varnado, Jr.,[a] Stephen Sproules,[b] Vincent M. Lynch,[a] and Christopher W. Bielawski*[a]

Abstract: High yielding syntheses of 1-(ferrocenylmethyl)-3-mesitylimidazolium iodide (**1**) and 1-(ferrocenylmethyl)-3-mesitylimidazol-2-ylidene (**2**) were developed. Complexation of **2** to [{Ir(cod)Cl}$_2$] (cod = *cis*,*cis*-1,5-cyclooctadiene) or [Ru(PCy$_3$)Cl$_2$(=CH-*o*-O-*i*PrC$_6$H$_4$)] (Cy = cyclohexyl) afforded **3** ([Ir(**2**)(cod)Cl]) and **5** ([Ru(**2**)Cl$_2$(=CH-*o*-O-*i*PrC$_6$H$_4$)]), respectively. Complex **4** ([Ir(**2**)(CO)$_2$Cl]) was obtained by bubbling carbon monoxide through a solution of **3** in CH$_2$Cl$_2$. Spectroelectrochemical IR analysis of **4** revealed that the oxidation of the ferrocene moiety in **2** significantly reduced the electron-donating ability of the *N*-heterocyclic carbene ligand (ΔTEP = 9 cm^{-1}; TEP = Tolman electronic parameter). The oxidation of **5** with [Fe(η^5-C$_5$H$_4$COMe)Cp][BF$_4$] as well as the subsequent reduction of the corresponding product [**5**][BF$_4$] with decamethylferrocene (Fc*) each proceeded in greater than 95% yield. Mössbauer, UV/Vis and EPR spectroscopy analysis confirmed that [**5**][BF$_4$] contained a ferrocenium species, indicating that the iron center was selectively oxidized over the ruthenium center. Complexes **5** and [**5**][BF$_4$] were found to catalyze the ring-closing metathesis (RCM) of diethyl diallylmalonate with observed pseudo-first-order rate constants (k_{obs}) of 3.1×10^{-4} and 1.2×10^{-5} s^{-1}, respectively. By adding suitable oxidants or reductants over the course of a RCM reaction, complex **5** was switched between different states of catalytic activity. A second-generation *N*-heterocyclic carbene that featured a 1′,2′,3′,4′,5′-pentamethylferrocenyl moiety (**10**) was also prepared and metal complexes containing this ligand were found to undergo iron-centered oxidations at lower potentials than analogous complexes supported by **2** (0.30–0.36 V vs. 0.56–0.62 V, respectively). Redox switching experiments using [Ru(**10**)Cl$_2$(=CH-*o*-O-*i*PrC$_6$H$_4$)] revealed that greater than 94% of the initial catalytic activity was restored after an oxidation–reduction cycle.

Keywords: ferrocene · homogeneous catalysis · olefin metathesis · redox-switchable catalysis · ruthenium · spectroelectrochemistry

Introduction

Redox-switchable catalysis (RSC) is a growing field of study that utilizes redox active ligands to influence the catalytic activities displayed by coordinated metals.[1] In a typical reaction (Scheme 1), a redox-switchable catalyst facilitates a given transformation (e.g., A→B) at a given rate, k_1, when the ligand on the catalyst is in a neutral state. However, upon oxidation or reduction, the activity or selectivity of the catalyst may change (i.e., $k_1 \neq k_2$), or the catalyst may facilitate a new transformation altogether (e.g., C→D). Such redox-switchable events frequently utilize a metallocene moiety to influence the ligand's electron-donating ability and, as a result, the catalytic activity displayed by the metal complex.[2] For example, in a seminal report, Wrighton elegantly demonstrated that a diphenylphosphinocobaltocene-ligated rhodium complex (**A**; see Figure 1) catalyzed the hydrogenation of cyclohexene faster than its oxidized cobaltocenium analogue; conversely, the oxidized complex was found to catalyze hydrosilylations faster than its neutral precursor.[3] Gibson and Long later reported a ferrocenyl-substituted titanium-based ring-opening polymerization catalyst (**B**) that showed a significantly decreased activity toward *rac*-lactide upon oxidation.[4] More recently, Diaconescu demonstrated that redox-switchable ferrocene-containing alkoxide (M = Y or Ce, R = *t*Bu) or aryloxide phosfen (M = In, R = Ph) complexes (**C**) may be used to control the ring-

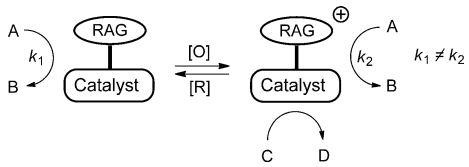

Scheme 1. General scheme for RSC. RAG = redox active group, [O] = oxidation, [R] = reduction, A and C = reactants, B and D = products and k_1, k_2 = rate constants.

[a] Dr. K. Arumugam, C. D. Varnado, Jr., Dr. V. M. Lynch, Prof. Dr. C. W. Bielawski
Department of Chemistry and Biochemistry
The University of Texas at Austin, Austin, TX 78712 (USA)
Fax: (+1) 512-471-8696
E-mail: bielawski@cm.utexas.edu

[b] Dr. S. Sproules
WestCHEM, School of Chemistry
University of Glasgow, Glasgow G12 8QQ (UK)

Supporting information for this article is available on the WWW under http://dx.doi.org/10.1002/chem.201301247.

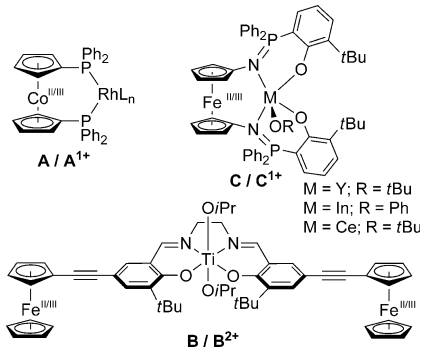

Figure 1. Representative examples of redox-switchable catalysts.

opening polymerization of L-lactide and trimethylene carbonate, respectively.[5]

Each of the aforementioned redox active ligands are multidentate, which contributes to the high stability of the corresponding complexes, but also imposes restrictions on the types of catalysts that may be synthesized with redox-switchable functionalities.[6] A general solution to this drawback may lie in the area of *N*-heterocyclic carbenes (NHCs), which are strongly coordinating, monodentate ligands[7] that have received widespread attention in broad range of applications,[8] particularly in organometallic catalysis.[9] Excellent examples of transformations that have benefitted from NHC-supported complexes include olefin metatheses,[10] hydrogenations,[11] and a sundry of coupling reactions.[6,12] An important subclass of NHCs are those that feature *N*-ferrocenyl groups, which are relatively straightforward to prepare, often display reversible electrochemistry, and coordinate to a wide range of transition metals.[13] Moreover, we and others have shown that the electron density at the metal centers ligated to *N*-ferrocenyl-substituted NHCs correlate with the oxidation state of the ferrocenyl unit.[13s,t,v,w] Since catalytic activity is often intimately tied to the electronic characteristics of ligated metals, RSC may provide new avenues for modulating the instrinsic chemo- and regioselectivities displayed by catalysts supported by redox-active NHCs. To explore the potential of ferrocene-containing NHCs in RSC, we describe herein a series of redox-switchable olefin metathesis catalysts and demonstrate their utility in controlling ring-closing metathesis (RCM) reactions.[14]

Results and Discussion

Our efforts began with the synthesis of a ferrocene-containing NHC in conjunction with a detailed study of the electron-donating ability of the ligand as a function of the oxidation state of the redox-active group. To facilitate key electrochemical and spectroscopic measurements, a series of Ir-based complexes that were supported by the aforementioned NHC ligand were prepared and evaluated. Ultimately, the results from these studies helped to rationalize the activity displayed by a first-generation redox-switchable olefin metathesis catalyst and guided the development of a second-generation derivative, which showed improved redox-switchable functions.

Following a modified literature procedure,[15] *N*-mesityl imidazole was alkylated with (ferrocenylmethyl)trimethylammonium iodide to afford **1** in 83% yield (Scheme 2). The

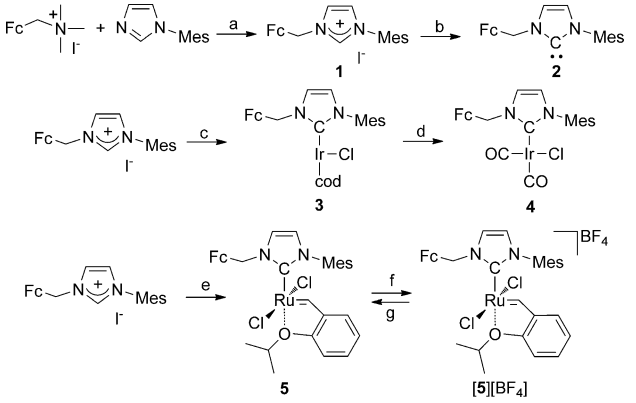

Scheme 2. Synthesis of **2** and various metal complexes (Fc = ferrocenyl, Mes = mesityl, cod = *cis,cis*-1,5-cyclooctadiene): a) CH_3CN, 80 °C, 24 h, 83% yield. b) NaHMDS (1 equiv), toluene, 25 °C, 1 h, 96% yield. c) i) NaHMDS (1 equiv), toluene, 25 °C, 1 h; ii) $[\{Ir(cod)Cl\}_2]$ (0.5 equiv), 25 °C, 12 h, 85% yield. d) CO (1 atm), CH_2Cl_2, 25 °C, 30 min, 92% yield. e) i) NaHMDS (1 equiv), toluene, 25 °C, 1 h; ii) $[Ru(PCy_3)Cl_2(=CH\text{-}o\text{-}O\text{-}iPrC_6H_4)]$ (0.9 equiv), 25 °C, 12 h, 62% yield f) $[Fe(\eta^5\text{-}C_5H_4COMe)Cp]\text{-}[BF_4]$ (1 equiv), CH_2Cl_2, 25 °C, 2 h, 90% yield. g) Decamethylferrocene (1 equiv), CH_2Cl_2, 25 °C, 1 h, 93% yield.

salient spectroscopic characteristics displayed by the isolated salt were consistent with the values reported for analogous compounds (e.g., the ^{1}H NMR chemical shift of the $C_{imidazolium}$–H group was recorded at δ = 9.48 ppm; $[D_6]$DMSO).[13g] Treatment of **1** with sodium hexamethyldisilazide (NaHMDS) in toluene afforded *N*-ferrocenylmethyl-*N'*-mesitylimidazol-2-ylidene (**2**), as evidenced by the absence of the imidazolium ^{1}H NMR signal in conjunction with the appearance of a diagnostic ^{13}C NMR signal at δ = 217.1 ppm (C_6D_6).[16] X-ray diffraction quality single crystals of **2** were grown from a saturated solution in toluene at −35 °C.[17] The solid-state structure of the free carbene (Figure 2) exhibited a longer average C1–N bond length and a contracted N1-C1-N2 bond angle than its imidazolium precursor (Figure S2 in the Supporting Information). Moreover, the pendant *N*-ferrocenylmethyl group was oriented toward the carbenoid nucleus (C1–Fe1 = 4.298 Å) in **2** yet away in **1** (C1–Fe1 = 5.246 Å), presumably due to differential packing effects. As free NHCs are known to ligate to metallocenes,[18] the isolation and solid-state elucidation of NHCs bearing *N*-ferrocenyl and *N*-ferrocenylmethyl groups is rare.[13w] Indeed, to the best of our knowledge, **2** is the first crystalline NHC bearing a pendant *N*-ferrocenyl group.

The introduction of free NHC **2** (generated in situ) to 0.5 equivalents of $[\{Ir(cod)Cl\}_2]$ in toluene led to the formation of **3** (Scheme 2), which was subsequently isolated in 85% yield by filtration. Bubbling CO through a solution of **3** in CH_2Cl_2 for 30 min, followed by purification of the resi-

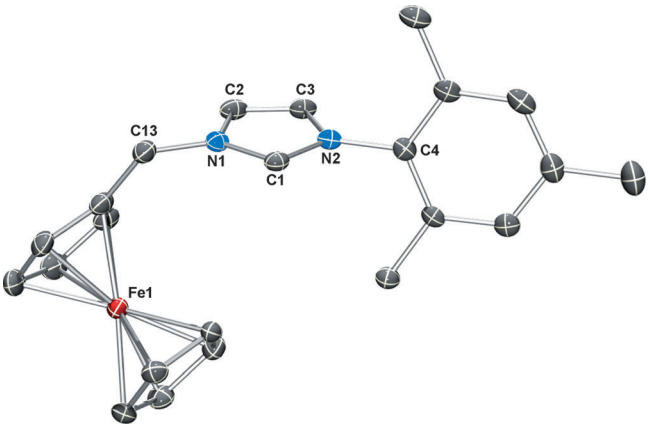

Figure 2. ORTEP diagram of **2** rendered using POV-Ray. Thermal ellipsoid plots were drawn at the 50% probability level. Hydrogen atoms and solvent molecules are omitted for clarity. Data are shown for one of two independent molecules in the asymmetric unit. Selected bond lengths [Å] and angles [°]: C1–N1 1.368(4), C1–N2 1.369(4), C2–N1 1.391(4), C3–N2 1.393(4), C2–C3 1.342(4), C4–N2 1.443(4), C13–N1 1.460(4), N1-C1-N2 101.9(2), N1-C13-C14 115.6(3).

due obtained upon evaporation using a series of *n*-pentane washes, afforded **4** in 93% yield. X-ray quality crystals of **3** and **4** were independently grown by slowly diffusing *n*-pentane into concentrated CH_2Cl_2 solutions of the complexes. As shown in Figures 3 and 4, the aforementioned Ir com-

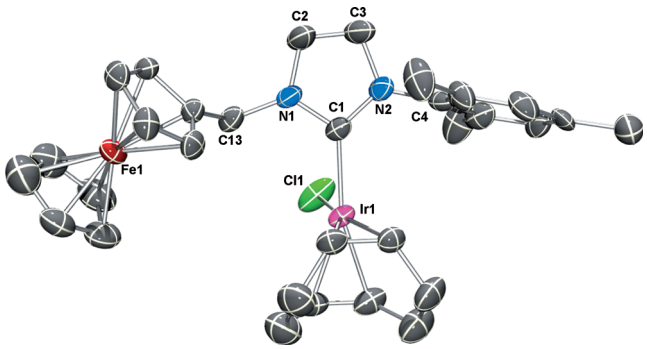

Figure 3. ORTEP diagram of **3** rendered using POV-Ray. Thermal ellipsoid plots were drawn at the 30% probability level. Hydrogen atoms are omitted for clarity. Selected bond lengths [Å] and angles [°]: C1–N1 1.363(11), C1–N2 1.356(12), C2–N1 1.382(13), C3–N2 1.396(12), C2–C3 1.354(15), C4–N2 1.461(13), C13–N1 1.441(12), C1–Ir1 2.041(9), Cl1–Ir1 2.358(3), N1-C1-N2 103.9(8), N1-C13-C14 112.2(8).

plexes adopted square-planar coordination geometries as expected for d^8 metals in strong ligand field environments. The N1-C1-N2 bond angles and the Ir1–C1 bond lengths measured in the solid-state structures of **3** and **4** are in good agreement with data reported for analogous compounds.[13v,19]

Next, efforts were directed toward the synthesis of Ru-based complexes bearing **2**.[10g–i,20] Due to their high stability and high catalytic activities in RCM reactions,[21] efforts were directed toward the synthesis of a Hoveyda–Grubbs type[22] (HG-type) analogue (i.e., **5**); an oxidized derivative

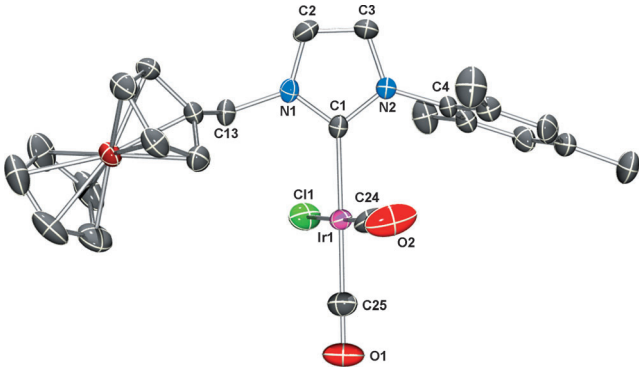

Figure 4. ORTEP diagram of **4** rendered using POV-Ray. Thermal ellipsoid plots were drawn at the 50% probability level. Hydrogen atoms are omitted for clarity. Selected bond lengths [Å] and angles [°]: C1–N1 1.350(5), C1–N2 1.363(5), C2–N1 1.372(5), C3–N2 1.382(5), C2–C3 1.336(6), C4–N2 1.444(5), C13–N1 1.483(5), C1–Ir1 2.070(4), Cl1–Ir1 2.3456(11), C24–Ir1 1.821(5), C25–Ir1 1.887(5), N1-C1-N2 104.5(3), N1-C13-C14 113.0(3).

([**5**][BF_4]) was also prepared for comparative purposes. Treatment of **1** with NaHMDS in toluene followed by filtration and subsequent addition of 0.9 equivalents [Ru(PCy_3)Cl_2(=CH-*o*-O-*i*PrC_6H_4)] to the filtrate lead to the formation of **5** (Scheme 2). The complex was isolated in 62% yield through precipitation from cold *n*-pentane (−35 °C) followed by filtration. Reflective of a more electron-rich environment at the metal center due to the incorporation of the strongly donating NHC ligand,[22a] the diagnostic alkylidene signal (Ru=CH_α) displayed by [Ru(PCy_3)Cl_2(=CH-*o*-O-*i*PrC_6H_4) at $\delta = 17.45$ ppm shifted to $\delta = 16.35$ ppm in **5** (CD_2Cl_2). X-ray diffraction quality single crystals of **5** were grown by slow vapor diffusion of *n*-pentane into a saturated solution of the complex in CH_2Cl_2. As shown in Figure 5, the structure of the complex adopted a distorted square-pyr-

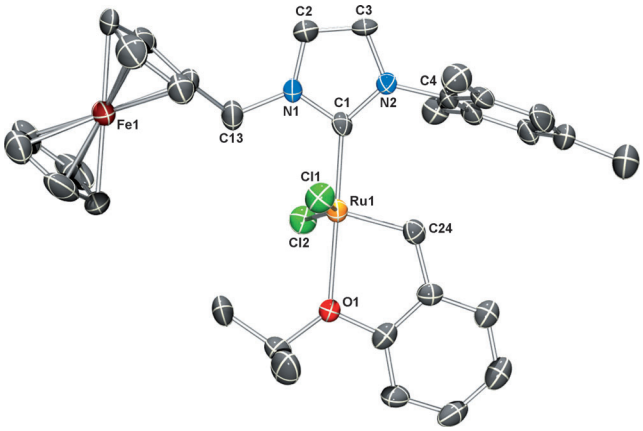

Figure 5. ORTEP diagram of **5** rendered using POV-Ray. Thermal ellipsoid plots were drawn at the 50% probability level. Hydrogen atoms are omitted for clarity. Selected bond lengths [Å] and angles [°]: C1–N1 1.353(7), C1–N2 1.369(7), C2–N1 1.382(7), C3–N2 1.384(7), C2–C3 1.333(8), C4–N2 1.456(7), C13–N1 1.482(7), Ru1–C1 1.980(6), Ru1–C24 1.822(6), Ru1–O1 2.261(4), Ru1–Cl1 2.3435(17), Ru1–Cl2 2.3571(17), N1-C1-N2 103.1(5), N1-C13-C14 113.3(5), Cl1-Ru1-Cl2 151.43(6), N2-C1-Ru1 135.8(5).

amidal geometry with the alkylidene unit oriented perpendicular to the C1-Ru1-Cl1-Cl2-O1 mean plane. The Cl1-Ru-Cl2 (151.42(6)°) and O1-Ru1-C1 (179.3(2)°) bond angles are in accord with data reported for other HG-type complexes.[22] Using a series of nuclear overhauser enhancement spectroscopy (NOESY) experiments, the solution-state structure (CD_2Cl_2) of the complex was determined to be similar to the structure observed in the solid state (see the Supporting Information). Treatment of **5** with acetylferrocenium tetrafluoroborate ([Fe(η^5-C_5H_4COMe)Cp][BF_4]) in CH_2Cl_2 followed by the addition of Et_2O afforded a dark green precipitate (90% yield), which was subsequently identified as [**5**][BF_4] by elemental analysis, electron paramagnetic resonance (EPR) and Mössbauer spectroscopy (see below). The complex [**5**][BF_4] was successfully reduced to **5** in CH_2Cl_2 using decamethylferrocene (Fc*) and the product was isolated in 95% yield, thus demonstrating that the two complexes were chemically interconvertable.

To measure the electronic properties of the aforementioned compounds, a series of electrochemical measurements were conducted in CH_2Cl_2 with [N(nBu$_4$)][PF_6] as the electrolyte; key data are summarized in Table 1 (see Figures 7 and S5–S9 in the Supporting Information for the corresponding cyclic voltammograms (CVs) and differential pulse voltammograms (DPVs)). Since the iodide counterion in **1** was found to undergo oxidation along with the ferrocenyl substituent, the analogous hexafluorophosphate salt **6** ([**2**H][PF_6]) was synthesized (by anion metathesis of **1** with [$CH_3CH_2)_3O$][PF_6]) and studied.[23] The CV of **6** revealed a single, reversible $Fe^{2+}\rightarrow Fe^{3+}$ oxidation process at 0.66 V (vs. saturated calomel electrode, SCE), which was comparable to the values reported in the literature for other *N*-ferrocenylimidazolium salts.[13g] In contrast, complex **3** exhibited two oxidation processes at 0.56 V and 0.96 V (vs. SCE), which were attributed to the Fe^{2+}/Fe^{3+} and Ir^{1+}/Ir^{2+} redox couples, respectively. While one reversible Fe^{2+}/Fe^{3+} couple was measured at 0.59 V (vs. SCE) for **4**, the corresponding Ir^{1+}/Ir^{2+} couple was not observed within the solvent window, likely due to the electron-withdrawing carbonyl groups present in the complex.

Table 1. Summary of the electrochemical data.[a]

Compound	$E_{1/2}$[b] [V]	$\Delta E_{1/2}$ [mV]
2	0.67 (qr)[c]	–
3	0.56 (r), 0.96 (ir)	400
4	0.59 (r)	–
5	0.62 (r), 1.01 (r)	370
6	0.66 (r)	–

[a] Data obtained by CV and DPV in CH_2Cl_2 with 0.10 M [N(nBu$_4$)][PF_6] electrolyte and referenced vs. SCE. [b] r = reversible, ir = irreversible, qr = quasi-reversible. [c] In THF (decomposition of **2** was observed in CH_2Cl_2).

Considering that the electron-donating abilities of NHCs may be conveniently monitored by measuring the carbonyl stretching frequencies (ν_{CO}) of NHC-supported [Ir(CO)$_2$Cl] complexes, subsequent efforts were directed toward probing the change in electron density at the Ir center in **4** upon oxidation of the ferrocene-containing ligand (i.e., **2**).[24] Compound **4** exhibited ν_{CO} bands at 2064 and 1980 cm^{-1}, which are intermediate of other NHC-supported [Ir(CO)$_2$Cl] complexes (*trans*: 2055–2072 cm^{-1}, *cis*: 1971–1989 cm^{-1}) reported in the literature.[13v,19f,g,25] The corresponding Tolman electronic parameter[26] (TEP) of **2** was calculated from the aforementioned ν_{CO} frequencies using an equation developed by Crabtree[27] and later modified by Nolan[19g] (TEP = $0.847\times\nu_{av}+336$ cm^{-1}) to be similar (2049 cm^{-1}) to the TEPs reported for 1,3-diadamantylimidazolylidene (2049.5 cm^{-1}) and 1,3-di(*tert*-butyl)-imidazolylidene (2050.1 cm^{-1}).[19g] Upon the bulk oxidation of **4** at 0.75 V (vs. SCE), an increase in the ν_{CO} frequencies was observed (Figure 6), which resulted in a significant increase in the calculated TEP (2058 cm^{-1}). As a point of reference, the TEP measured for oxidized **2** (i.e., **2**$^+$) was greater than the analogous value calculated for tricyclohexylphosphine (2056.4 cm^{-1}).[19g] Regardless, the result suggested to us that **2** may be switched between two different states of ligand-donating ability by changing the oxidation state of the ferrocenyl unit.

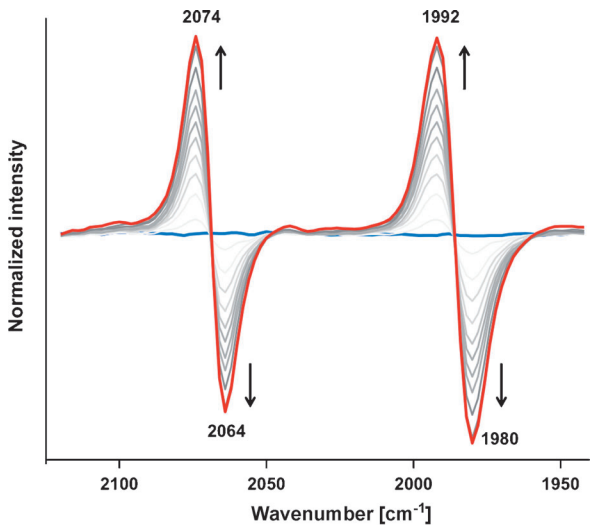

Figure 6. Normalized IR difference spectra showing the shift in the ν_{CO} frequencies upon oxidation (E_{app} = +0.75 V) of **4** ([**4**]$_0$ = 1 mM) in CH_2Cl_2 with 0.1 M [N(nBu$_4$)][PF_6] as the supporting electrolyte. The arrows indicate the direction of the spectral changes over time.

Building on the aforementioned results, the electrochemistry of the HG-type complex **5** was probed and found to exhibit two reversible oxidation processes at 0.62 V and 1.01 V (vs. SCE, Figure 7). The first oxidation was assigned to the Fe^{2+}/Fe^{3+} couple, while the second oxidation was attributed to a Ru^{2+}/Ru^{3+} oxidation process (vide infra). To gain additional insight into the electronic structure of **5**$^+$, controlled-potential coulometry at 0.75 V (vs. SCE) with concomitant UV/Vis absorption spectroscopy was performed. As shown in Figure 8, new absorption maxima near 239 nm and about 600 nm were observed for the first oxidation process. The band at around 600 nm has been previously ascribed to the formation of a ferrocenium (Fc$^+$) species.[28] After the for-

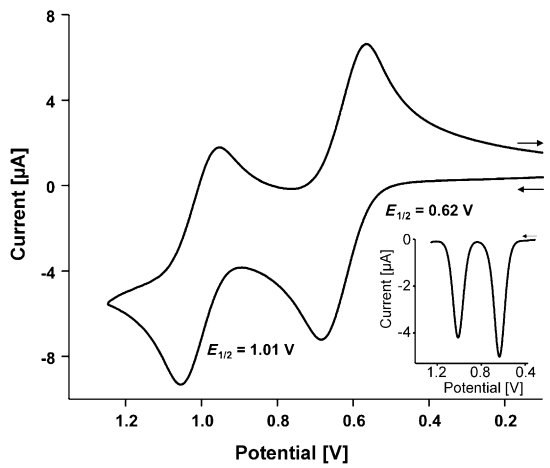

Figure 7. Cyclic voltammogram of **5** in CH_2Cl_2 with 1 mM of analyte and 0.1 M $[N(nBu_4)][PF_6]$, scan rate 100 mV s^{-1}. Inset: the differential pulse voltammogram of **5** under identical conditions (50 mV pulse amplitude).

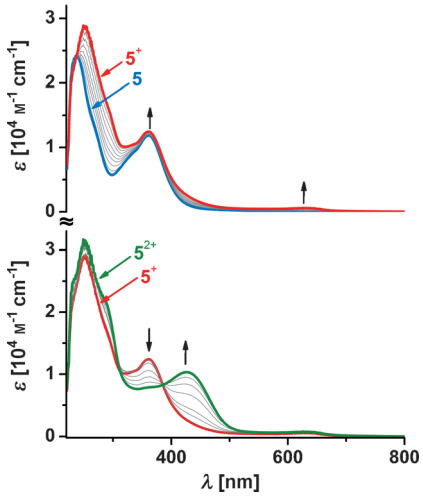

Figure 8. Electronic absorption spectra recorded during the bulk oxidation of **5**→**5**$^{1+}$ (top) (E_{app} = +0.75 V) and **5**$^{1+}$→**5**$^{2+}$ (bottom) (E_{app} = +1.2 V) in CH_2Cl_2 with 0.1 M $[N(nBu)_4][PF_6]$ as the supporting electrolyte at −25 °C. The arrows indicate the direction of the spectral changes over time.

mation of **5**$^+$ from **5** was complete, controlled-potential coulometry was performed at 1.2 V (vs. SCE) to generate **5**$^{2+}$. A new band at 426 nm ($\varepsilon = 1.03\times10^4$ M^{-1}cm^{-1}), consistent with the oxidation of $Ru^{2+}\rightarrow Ru^{3+}$, was observed.[29]

To support the electrochemical and spectroelectrochemical UV/Vis assignments, a series of electron paramagnetic resonance (EPR) and Mössbauer spectroscopy experiments were performed. After oxidizing **5** with acetylferrocenium tetrafluoroborate ($[Fe(\eta^5\text{-}C_5H_4COMe)Cp][BF_4]$), the EPR spectrum of the corresponding product [**5**][BF_4] was recorded in a dichloromethane/toluene glass at 5 K. As shown in Figure 9, the EPR spectrum revealed a sharp feature at $g_{||}$ = 4.24, a result consistent with the presence of a ferrocenium species.[28b,30] Moreover, the broadening of the $g_\perp$ feature was successfully modeled by including a large g-strain value (σ = 0.42) in the simulation to account for the micro-

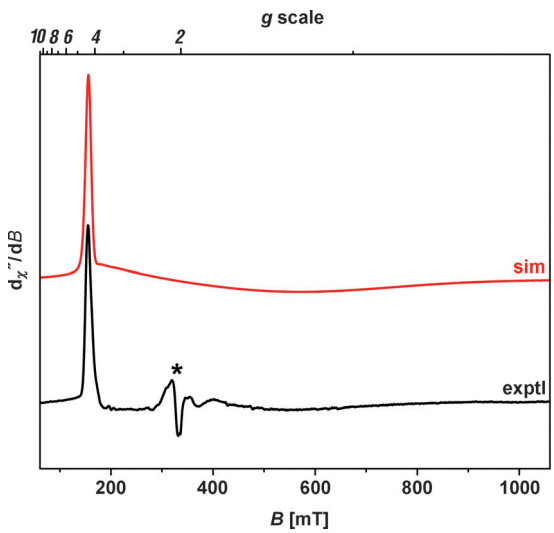

Figure 9. X-band EPR spectrum of **5**$^+$ (black line) in a CH_2Cl_2/toluene solution at 5 K and corresponding simulation (red line). Experimental conditions: frequency, 9.4361 GHz; power, 0.63 mW; modulation, 3.0 mT. Simulation parameters: g = 4.24, 1.29, 1.29; W = 110, 500, 500 × 10^{-4} cm^{-1}; g-strain, σ_x = 0.42. The asterisk denotes a Ru^{3+} impurity that accounted for < 1 % of the total signal intensity.

heterogeneity in the frozen glass. The line broadening was believed to arise from the bulky pendent arm of the Fe-containing group, which challenged an ability to observe the $g_\perp$ in the EPR spectrum of **5**$^+$. However, the formation of a ferrocenium species was supported by the large g anisotropy ($\Delta g = g_{||} - g_\perp$ = 2.95), which stems from the unquenched orbital angular momentum within the degenerate $^2E_{2g}$ ground state. Since this g anisotropy cannot be generated by a Ru^{3+} d^5 ion ($S = {}^1/_2$) in this ligand field nor to a quartet ($S = {}^3/_2$) ground state, the signals were assigned as described above.

To further support the notion that the ferrocenyl unit in **5** underwent oxidation upon the addition of $[Fe(\eta^5\text{-}C_5H_4COMe)Cp][BF_4]$, **5** and [**5**]$BF_4$ were independently analyzed using Mössbauer spectroscopy. As shown in Figure 10,[31] complex **5** is characterized by an isomer shift at δ = 0.50 mm s^{-1} and a large quadrupole splitting at ΔE_Q = 2.31 mm s^{-1}, which is consistent with the low-spin Fe^{2+} d^6 center of ferrocene. The oxidized product **5**$^+$ exhibits the same isomer shift, but the quadrupole splitting collapses to ΔE_Q = 0.13 mm s^{-1}, a value characteristic of a ferrocenium species.[31] Collectively, the electronic absorption, EPR, and Mössbauer spectra revealed that the first oxidation process is ferrocene-based.

Having evaluated the ligand-donating ability of **2** as a function of its oxidation state, efforts were directed toward exploring the utility of the latter in RSC. Using a modified literature procedure,[32] the ring-closing metathesis (RCM) of diethyl diallylmalonate (**7**) ([**7**]$_0$ = 0.1 M) to its respective cyclic product (**8**) was monitored by ^{1}H NMR spectroscopy at 30 °C in CD_2Cl_2 using 1 mol % **5** or [**5**][BF_4] as the catalyst; see Equation (1). As shown in Figure 11, an 80 % conversion of starting material to product was observed within 1 h when **5** was employed as the catalyst and the corre-

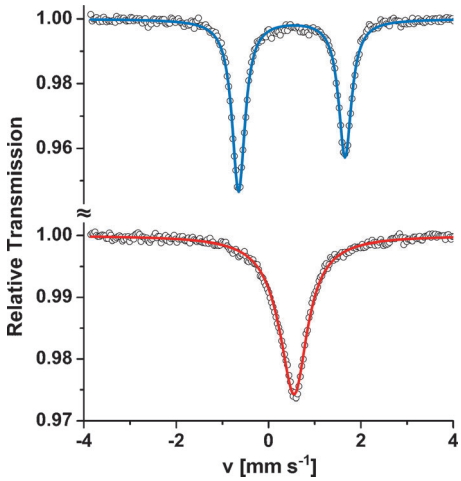

Figure 10. Zero-field Mössbauer spectra of **5** (blue, top) and [**5**][BF_4] (red, bottom) recorded using solid samples at 80 K. The open circles reflect the experimental data; the solid lines are the corresponding spectral fits.

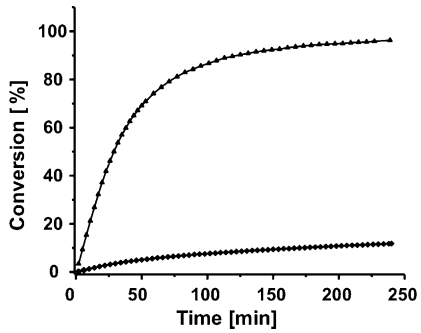

Figure 11. Plots of the percent conversion of **7** to **8** versus time as catalyzed by 1 mol% of **5** (triangles) or [**5**][BF_4] (diamonds). Conditions: $[\mathbf{7}]_0 = 0.1$ M, CD_2Cl_2, 30 °C.

sponding pseudo-first-order rate constant (k_{obs}) was calculated to be 3.1×10^{-4} s^{-1}. In contrast, the analogous reaction involving [**5**][BF_4] was measured to be significantly slower ($k_{obs} = 1.2\times10^{-5}$ s^{-1}) and the catalyst converted only 7% of **7** to **8** after 1 h. We hypothesized that the oxidation of the ferrocene moiety ($Fe^{2+}\rightarrow Fe^{3+}$) in complex **5** reduced the electron density at the ligated metal center and attenuated the catalytic activity accordingly.[10i]

Building on the observation that **5** and [**5**][BF_4] catalyzed the RCM of **7** with different rate constants, subsequent efforts were directed toward modulating the activity of the catalyst over the course of a reaction. Following the addition of **5** (1 mol%) to a CD_2Cl_2 solution of **7** ($[\mathbf{7}]_0 = 0.1$ M), the resulting mixture was monitored at 30 °C by ^{1}H NMR spectroscopy (see Figure 12). After 10 min (ca. 16% conversion of **7** to **8**; $k_{obs} = 3.0\times10^{-4}$ s^{-1}), one equivalent (with respect to **5**) of a chemical oxidant, [Fe(η^5-$C_5H_4COCH_3$)Cp][BF_4], was added to the reaction mixture. The addition resulted in the solution changing color from yellow to brown and was accompanied by a significant decrease in catalytic activity ($k_{obs} = 0.98\times10^{-5}$ s^{-1}), consistent with the in situ conversion of **5**→**5**$^+$. Subsequent addition of 1.1 equivalents (with respect to **5**) of a chemical reductant, decamethylferrocene (Fc*), to the mixture restored the initial yellow color and the relatively high catalytic activity ($k_{obs} = 3.8\times10^{-5}$ s^{-1}). As shown in Figure 12 (bottom), the aforementioned switching cycle was successfully repeated multiple times over the course of a single reaction.[33,34]

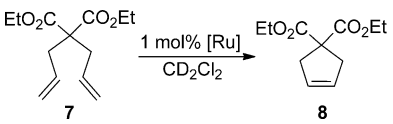

(1)

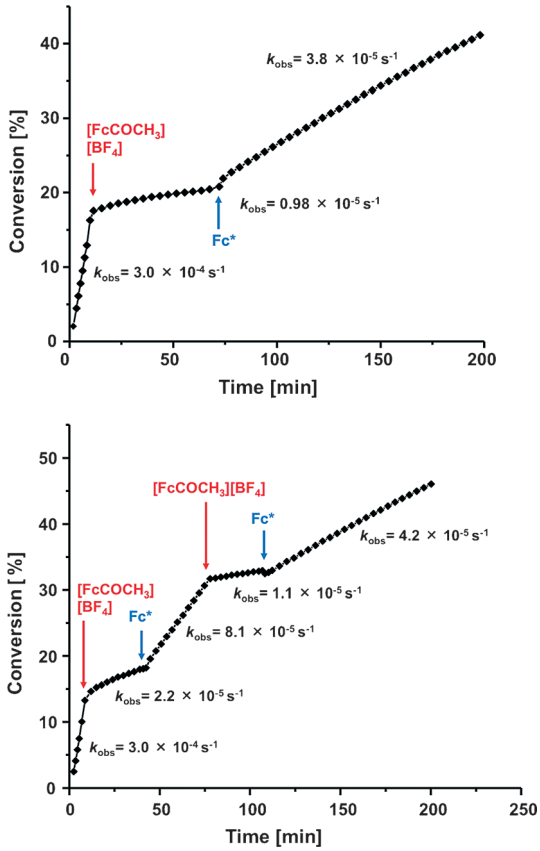

Figure 12. Plots of the percent conversion of **7** to **8** versus time as catalyzed by 1 mol% of **5**; conditions: $[\mathbf{7}]_0 = 0.1$ M, CD_2Cl_2, 30 °C. The arrows indicate the time at which one equivalent of said reagent with respect to **5** was added. The corresponding rate constants over the given periods of time are indicated.

Close inspection of the redox-switching data summarized in Figure 12 revealed that only about 13% of the initial catalytic activity, as determined by the respective rate constants, was successfully restored.[35] Considering that the oxidation potentials of the iron and ruthenium centers in **5** differed by only 380 mV, we attributed the attenuated activity to partial ruthenium oxidation, which led to premature catalyst decomposition. To develop a more robust catalyst, efforts were directed towards incorporating a 1′,2′,3′,4′,5′-pen-

tamethylferrocene (Me_5Fc) moiety into an NHC scaffold, which was expected[36] to undergo oxidation at about 300 mV lower potential than the parent ferrocene analogue.

As summarized in Scheme 3, treatment of 1′,2′,3′,4′,5′-pentamethylferrocenylmethanol[37] with HBF_4 in the presence of mesitylimidazole led to formation of the imidazolium salt **9** as a crystalline product.[13u,36] In order to evaluate and compare electron-donating ability of the corresponding NHC (i.e., **10**) to **2**, the iridium complex **11** was prepared in a similar manner to that described for the synthesis of **3** and subjected to electrochemical analysis.

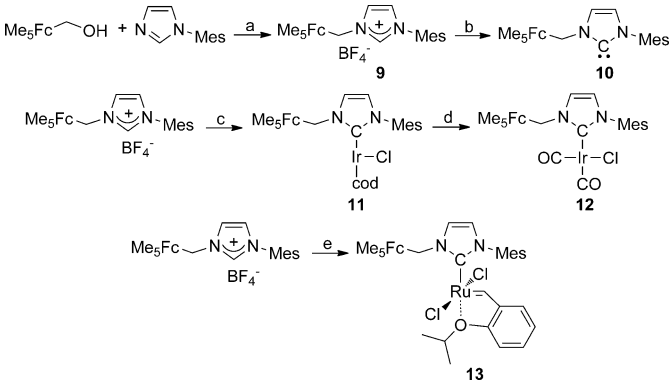

Scheme 3. Synthesis of **10** and various metal complexes (Me_5Fc = 1′,2′,3′,4′,5′-pentamethylferrocene). a) i) HBF_4, CH_2Cl_2, 1 min; ii) *N*-mesitylimidazole, 12 h, 41% yield. b) NaHMDS (1 equiv), benzene, 1 h. c) i) NaHMDS (1 equiv), benzene, 25 °C, 15 min; ii) $[\{Ir(cod)Cl\}_2]$ (0.5 equiv), 25 °C, 12 h, 79% yield. d) CO (1 atm), CH_2Cl_2, 25 °C, 2 h, 82% yield. e) i) NaHMDS (1 equiv), toluene, 25 °C, 30 min; ii) $[Ru(PCy_3)Cl_2(=CH\text{-}o\text{-}O\text{-}iPrC_6H_4)]$ (0.5 equiv), 25 °C, 3 h; iii) S_8 (2 equiv), 12 h, 48% yield.

Cyclic voltammetry of **11** (Figure S10 in the Supporting Information) in CH_2Cl_2 in the presence of $[N(nBu_4)][PF_6]$ as the electrolyte revealed that the iron-centered oxidation process occurred at 0.30 V (vs. SCE), which corresponded to a 260 mV cathodic shift as compared to the analogous oxidation process exhibited by **3**. However, the iridium oxidation processes displayed by **3** and **11** were found to occur at similar potentials (cf., 0.96 V vs. 0.97 V, respectively), which suggested to us that even though the Me_5Fc-containing ligand (**10**) underwent oxidation at a lower overall potential than its Fc parent (**2**), there was minimal difference in the donating ability of the two ligands.

To further characterize the steric and electronic properties of **10**, the complex **12** (i.e., [Ir(**10**)$(CO)_2$Cl]) was prepared by stirring a solution of **11** under an atmosphere of CO (g) and isolated by precipitation. X-ray diffraction analysis of single crystals grown by the slow diffusion of *n*-pentane into a saturated solution of **12** in chloroform were in accord with the recorded spectroscopic data and confirmed the identity of this complex (Figure S4 in the Supporting Information). As expected, **12** exhibited a square-planar geometry with bond lengths and bond angles comparable to those measured in the solid-state structure of **4**. Likewise, the percent buried volumes, a measure of steric bulk, displaced by ligands **2** and **10** were calculated to be similar (29.4% vs. 31.5%, respectively) using Cavallo's method.[38]

With complex **12** in hand, the electron-donating ability of **10** was measured and compared to that of **2**. The ν_{CO} frequencies displayed by **12** were recorded at 2064 and 1979 cm^{-1}, and were nearly identical to those measured for **4**. Likewise, the TEP value of **10** (2048 cm^{-1}) was calculated to be similar to that of **2** (2049 cm^{-1}). The CV of **12** (Figure S11 in the Supporting Information) revealed that the first oxidation process occurs at 0.34 V (vs. SCE; Table 2), which is 250 mV cathodically shifted when compared to the analogous process displayed by **4**. Even though the ligand oxidation occurred at lower potential, the resulting TEP difference between **12** and $\mathbf{12}^+$ is nearly identical to that measured between **2** and $\mathbf{2}^+$ (cf., 8 vs. 9 cm^{-1}, respectively), as determined by a spectroelectrochemical experiment (Figure S13 in the Supporting Information).

Table 2. Summary of the electrochemical data.[a]

Compound	$E_{1/2}$[b] [V]	$\Delta E_{1/2}$ [mV]
11	0.30 (r), 0.97 (ir)	670
12	0.34 (r)	–
13	0.36 (r), 1.02 (r)	660

[a] Data obtained by CV and DPV in CH_2Cl_2 with 0.10 M $[N(nBu_4)][PF_6]$ electrolyte and referenced vs. SCE. [b] r = reversible, ir = irreversible.

To test the performance of **10** in RSC, Ru complex **13** was prepared in an analogous manner to **5**. Unfortunately, treating **10** with $[Ru(PCy_3)Cl_2(=CH\text{-}o\text{-}O\text{-}iPrC_6H_4)]$ yielded a mixture of products, one of which was a complex in which the phosphine ligand was coordinated to the Ru center, yet the isopropyloxy group was dissociated, as evidenced by diagnostic ^1H NMR (a doublet at $\delta = 20.95$ ppm and a singlet at $\delta = 16.68$ ppm) and ^{31}P NMR ($\delta = 23.5$ and 10.9 ppm) signals. To maximize the yield of **13**, the aforementioned reaction mixture was stirred with two equivalents of elemental sulfur, an effective phosphine scavenger,[39] followed by silica column chromatography under an inert atmosphere which afforded the desired complex as a yellow solid in 48% isolated yield. X-ray quality crystals of **13** were obtained as red needles by vapor diffusion of pentane into a saturated solution of the complex in benzene. The solid-state structure of **13** exhibits a distorted square-pyramidal geometry with bond lengths and angles similar to those measured for the analogous solid-state structure of **5** (Figure 13).

The CV of **13** (Figure S12 in the Supporting Information) revealed an iron-centered oxidation at 0.36 V, corresponding to a 260 mV cathodic shift relative to the analogous oxidation process displayed by **5**. Consequently, the redox window measured between the Fe and Ru-centered oxidation processes exhibited by **13** was broadened to 660 mV, as opposed to the 380 mV window displayed by **5**. The wider electrochemical window facilitated the use of a weaker oxi-

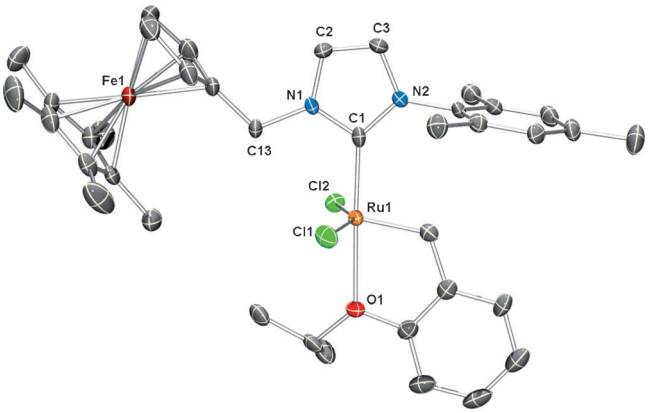

Figure 13. ORTEP diagram of **13** rendered using POV-Ray. Thermal ellipsoid plots were drawn at the 50% probability level. Hydrogen atoms are omitted for clarity. Selected bond lengths [Å] and angles [°]: C1–N1 1.364(4), C1–N2 1.368(4), C2–N1 1.382(4), C3–N2 1.393(4), C2–C3 1.340(5), C4–N2 1.443(4), C13–N1 1.479(4), Ru1–C1 1.988(4), Ru1–C29 1.822(4), Ru1–O1 2.277(2), Ru1–Cl1 2.3432(12), Ru1–Cl2 2.3287(11), N1-C1-N2 103.8(3), N1-C13-C14 111.6(3), Cl1-Ru1-Cl2 149.82(4), N2-C1-Ru1 134.7(3).

dant (i.e., [Fc][BF_4]; $E_{1/2}=0.475$ V in CH_2Cl_2 vs. SCE)[40] to oxidize **13**.

A ring-closing reaction was initiated by adding **13** (1 mol%) to a solution of **7** in CD_2Cl_2 ([**7**]$_0$=0.1 M) and monitored at 30 °C by ^{1}H NMR spectroscopy. As shown in Figure 14, the neutral complex catalyzed the reaction with a rate constant (k_{obs}) of 4.5×10^{-5} s^{-1}. However, upon oxidation with [Fc][BF_4], the rate constant was reduced to 0.86×10^{-5} s^{-1}. While the aforementioned rate constants are similar to those measured for **5** and **5**$^+$ respectively, the subsequent addition of decamethylferrocene to the in situ generated **13**$^+$ restored greater than 94% of the catalytic activity displayed by its neutral precursor ($k_{obs}=4.25\times10^{-5}$ s^{-1}).

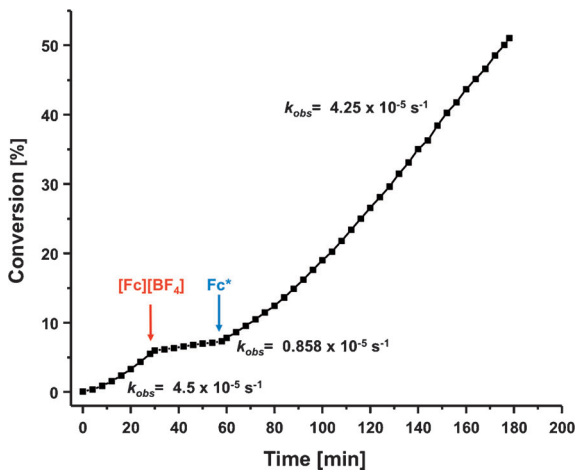

Figure 14. Plots of the percent conversion of **7** to **8** versus time as catalyzed by 1 mol% of **13**, conditions: [**7**]$_0$=0.1 M, CD_2Cl_2, 30 °C. The arrows indicate the time at which one equivalent of said reagent with respect to **13** was added. The corresponding rate constants over the given periods of time are indicated.

Conclusions

In summary, we have developed straightforward syntheses of NHCs that feature redox-active *N*-ferrocenyl substituents and ligated these compounds to a series of iridium and catalytically active ruthenium complexes. By measuring the ν_{CO} frequencies of [Ir(**2**)(CO)$_2$Cl], the ligand-donating ability of the NHC **2** was found to decrease (ΔTEP=9 cm^{-1}) upon selective oxidation of the ferrocene moiety. Electrochemical analysis of **5** (i.e., [Ru(**2**)Cl$_2$(=CH-*o*-O-*i*PrC$_6$H$_4$)]) revealed two successive one-electron oxidations, corresponding to $Fe^{2+}\rightarrow Fe^{3+}$ followed by $Ru^{2+}\rightarrow Ru^{3+}$, respectively, as confirmed using a series of electrochemical, spectroelectrochemical UV/Vis absorption Mössbauer and EPR experiments. Complexes **5** and [**5**][BF_4] were found to catalyze the ring-closing metathesis (RCM) of diethyl diallylmalonate (**7**) at 30 °C, but at significantly different rates. Moreover, while the RCM reaction catalyzed by **5** was successfully attenuated through the addition of a chemical oxidant, the catalytic activity was only partial restored (ca. 13%) upon subsequent chemical reduction, presumably due to premature catalyst decomposition. Regardless, these results corroborated the hypothesis that the oxidation of the ligand in **5** afforded a complex with diminished electron density at the metal center and therefore reduced catalytic activity. To increase the robustness of the catalyst and to improve its redox-switchable functions, an NHC bearing a 1′,2′,3′,4′,5′-pentamethylferrocene substituent was prepared (**10**). Complexes supported by **10** were found to oxidize at potentials that were at least 250 mV lower than the analogues that contained the parent ferrocene moieties. Moreover, more than 94% of the initial RCM activity displayed by a Ru-based olefin metathesis catalyst supported by **10** was restored after a full redox-switching cycle. To the best of our knowledge, these are the first homogeneous, redox-switchable, NHC-supported Ru catalysts that have been used to control RCM through changes in ligand electronics. More broadly, the results presented herein are expected to guide the development of other olefin metathesis and other NHC-supported catalysts, the intrinsic chemo- and regioselectivities of which are determined by the oxidation state of the redox-switchable ligand.

Acknowledgements

This material is based upon work supported in part by the U. S. Army Research Laboratory under grant number W911NF-09-1-0446. Additional support from the National Science Foundation (CHE-1266323 and CHE-0741973) and the Robert A. Welch Foundation (F-0046) is also acknowledged. We thank Steve Sorey for his assistance with the NMR experiments. Support from the EPSRC National UK EPR Facility and Service is gratefully acknowledged.

[1] A. M. Allgeier, C. A. Mirkin, *Angew. Chem.* **1998**, *110*, 936–952; *Angew. Chem. Int. Ed.* **1998**, *37*, 894–908.
[2] I. M. Lorkovic, M. S. Wrighton, W. M. Davis, *J. Am. Chem. Soc.* **1994**, *116*, 6220–6228.

[3] I. M. Lorkovic, R. R. Duff, M. S. Wrighton, *J. Am. Chem. Soc.* **1995**, *117*, 3617–3618.

[4] C. K. A. Gregson, V. C. Gibson, N. J. Long, E. L. Marshall, P. J. Oxford, A. J. P. White, *J. Am. Chem. Soc.* **2006**, *128*, 7410–7411.

[5] a) E. M. Broderick, N. Guo, C. S. Vogel, C. Xu, J. Sutter, J. T. Miller, K. Meyer, P. Mehrkhodavandi, P. L. Diaconescu, *J. Am. Chem. Soc.* **2011**, *133*, 9278–9281; b) E. M. Broderick, N. Guo, T. Wu, C. S. Vogel, C. Xu, J. Sutter, J. T. Miller, K. Meyer, T. Cantat, P. L. Diaconescu, *Chem. Commun.* **2011**, *47*, 9897–9899.

[6] The coupling activities displayed by 1,4-naphthoquinone annulated *N*-heterocyclic carbene supported Group 10 metal complexes may be controlled by varying the oxidation state of the redox-active NHC ligand; see: A. G. Tennyson, V. M. Lynch, C. W. Bielawski, *J. Am. Chem. Soc.* **2010**, *132*, 9420–9429.

[7] a) D. Martin, M. Melaimi, M. Soleilhavoup, G. Bertrand, *Organometallics* **2011**, *30*, 5304–5313; b) R. Tonner, G. Heydenrych, G. Frenking, *Chem. Asian J.* **2007**, *2*, 1555–1567.

[8] a) P. L. Arnold, I. J. Casely, *Chem. Rev.* **2009**, *109*, 3599–3611; b) O. Back, B. Donnadieu, P. Parameswaran, G. Frenking, G. Bertrand, *Nat. Chem.* **2010**, *2*, 369–373; c) A. J. Boydston, K. A. Williams, C. W. Bielawski, *J. Am. Chem. Soc.* **2005**, *127*, 12496–12497; d) Y. Chi, P. T. Chou, *Chem. Soc. Rev.* **2010**, *39*, 638–655; e) D. J. Coady, D. M. Khramov, B. C. Norris, A. G. Tennyson, C. W. Bielawski, *Angew. Chem.* **2009**, *121*, 5289–5292; *Angew. Chem. Int. Ed.* **2009**, *48*, 5187–5190; f) F. E. Hahn, M. C. Jahnke, *Angew. Chem.* **2008**, *120*, 3166–3216; *Angew. Chem. Int. Ed.* **2008**, *47*, 3122–3172; g) J. C. Y. Lin, R. T. W. Huang, C. S. Lee, A. Bhattacharyya, W. S. Hwang, I. J. B. Lin, *Chem. Rev.* **2009**, *109*, 3561–3598; h) J. D. Masuda, W. W. Schoeller, B. Donnadieu, G. Bertrand, *J. Am. Chem. Soc.* **2007**, *129*, 14180–14181; i) B. C. Norris, C. W. Bielawski, *Macromolecules* **2010**, *43*, 3591–3593; j) D. Scheschkewitz, *Angew. Chem.* **2008**, *120*, 2021–2023; *Angew. Chem. Int. Ed.* **2008**, *47*, 1995–1997; k) R. Wolf, W. Uhl, *Angew. Chem.* **2009**, *121*, 6905–6907; *Angew. Chem. Int. Ed.* **2009**, *48*, 6774–6776.

[9] a) S. Díez-González, N. Marion, S. P. Nolan, *Chem. Rev.* **2009**, *109*, 3612–3676; b) D. Enders, O. Niemeier, A. Henseler, *Chem. Rev.* **2007**, *107*, 5606–5655; c) F. Glorius in *N-Heterocyclic Carbenes in Transition Metal Catalysis, Vol. 21*, Springer, Amsterdam, **2007**, pp. 1–20; d) M. He, J. W. Bode, *J. Am. Chem. Soc.* **2008**, *130*, 418–419; e) N. E. Kamber, W. Jeong, R. M. Waymouth, R. C. Pratt, B. G. G. Lohmeijer, J. L. Hedrick, *Chem. Rev.* **2007**, *107*, 5813–5840; f) E. M. Phillips, M. Wadamoto, A. Chan, K. A. Scheidt, *Angew. Chem.* **2007**, *119*, 3167–3170; *Angew. Chem. Int. Ed.* **2007**, *46*, 3107–3110; g) J. R. de Alaniz, T. Rovis, *J. Am. Chem. Soc.* **2005**, *127*, 6284–6289; h) W. J. Sommer, M. Weck, *Coord. Chem. Rev.* **2007**, *251*, 860–873.

[10] a) M. Bieniek, C. Samojłowicz, V. Sashuk, R. Bujok, P. Śledź, N. L. Lugan, G. Lavigne, D. Arlt, K. Grela, *Organometallics* **2011**, *30*, 4144–4158; b) I. Fernández, N. Lugan, G. Lavigne, *Organometallics* **2012**, *31*, 1155–1160; c) A. Fürstner, *Angew. Chem.* **2000**, *112*, 3140–3172; *Angew. Chem. Int. Ed.* **2000**, *39*, 3012–3043; d) R. H. Grubbs, T. M. Trnka, *Ruthenium-Catalyzed Olefin Metathesis*, Wiley-VCH, Weinheim, **2005**; e) L. Jafarpour, S. P. Nolan, *J. Organomet. Chem.* **2001**, *617*, 17–27; f) T. Weskamp, W. C. Schattenmann, M. Spiegler, W. A. Herrmann, *Angew. Chem.* **1998**, *110*, 2631–2633; *Angew. Chem. Int. Ed.* **1998**, *37*, 2490–2493; g) J. Huang, E. D. Stevens, S. P. Nolan, J. L. Petersen, *J. Am. Chem. Soc.* **1999**, *121*, 2674–2678; h) M. Scholl, S. Ding, C. W. Lee, R. H. Grubbs, *Org. Lett.* **1999**, *1*, 953–956; i) T. M. Trnka, R. H. Grubbs, *Acc. Chem. Res.* **2001**, *34*, 18–29.

[11] a) A. C. Hillier, H. M. Lee, E. D. Stevens, S. P. Nolan, *Organometallics* **2001**, *20*, 4246–4252; b) H. M. Lee, T. Jiang, E. D. Stevens, S. P. Nolan, *Organometallics* **2001**, *20*, 1255–1258; c) L. D. Vázquez-Serrano, B. T. Owens, J. M. Buriak, *Chem. Commun.* **2002**, 2518–2519; d) L. D. Vázquez-Serrano, B. T. Owens, J. M. Buriak, *Inorg. Chim. Acta* **2006**, *359*, 2786–2797; e) G. E. Dobereiner, A. Nova, N. D. Schley, N. Hazari, S. J. Miller, O. Eisenstein, R. H. Crabtree, *J. Am. Chem. Soc.* **2011**, *133*, 7547–7562.

[12] a) A. Correa, N. Marion, L. Fensterbank, M. Malacria, S. P. Nolan, L. Cavallo, *Angew. Chem.* **2008**, *120*, 730–733; *Angew. Chem. Int. Ed.* **2008**, *47*, 718–721; b) M. R. Fructos, T. R. Belderrain, P. de Frémont, N. M. Scott, S. P. Nolan, M. M. Díaz-Requejo, P. J. Pérez, *Angew. Chem.* **2005**, *117*, 5418–5422; *Angew. Chem. Int. Ed.* **2005**, *44*, 5284–5288; c) A. Gimeno, M. Medio-Simon, C. R. de Arellano, G. Asensio, A. B. Cuenca, *Org Lett.* **2010**, *12*, 1900–1903; d) R. E. Kinder, Z. Zhang, R. A. Widenhoefer, *Org. Lett.* **2008**, *10*, 3157–3159; e) N. Marion, P. de Fremont, G. Lemiere, E. D. Stevens, L. Fensterbank, M. Malacria, S. P. Nolan, *Chem. Commun.* **2006**, 2048–2050; f) S. P. Nolan, *Acc. Chem. Res.* **2011**, *44*, 91–100; g) M. G. Organ, M. Abdel-Hadi, S. Avola, N. Hadei, J. Nasielski, C. J. O'Brien, C. Valente, *Chem. Eur. J.* **2007**, *13*, 150–157; h) H. Seo, B. P. Roberts, K. A. Abboud, K. M. Merz, Jr., S. Hong, *Org Lett.* **2010**, *12*, 4860–4863; i) E. A. B. Kantchev, C. J. O'Brien, M. G. Organ, *Angew. Chem.* **2007**, *119*, 2824–2870; *Angew. Chem. Int. Ed.* **2007**, *46*, 2768–2813; j) C. J. O'Brien, E. A. B. Kantchev, C. Valente, N. Hadei, G. A. Chass, A. Lough, A. C. Hopkinson, M. G. Organ, *Chem. Eur. J.* **2006**, *12*, 4743–4748.

[13] a) A. J. Arduengo, T. P. Bannenberg, D. Tapu, W. J. Marshall, *Tetrahedron Lett.* **2005**, *46*, 6847–6850; b) A. J. Arduengo III, T. P. Bannenberg, D. Tapu, W. J. Marshall, *Chem. Lett.* **2005**, *34*, 1010–1011; c) A. J. Arduengo III, L. I. Iconaru, *Dalton Trans.* **2009**, 6903–6914; d) A. J. Arduengo, D. Tapu, W. J. Marshall, *J. Am. Chem. Soc.* **2005**, *127*, 16400–16401; e) A. J. Arduengo, D. Tapu, W. J. Marshall, *Angew. Chem.* **2005**, *117*, 7406–7410; *Angew. Chem. Int. Ed.* **2005**, *44*, 7240–7244; f) A. Bertogg, F. Camponovo, A. Togni, *Eur. J. Inorg. Chem.* **2005**, 347–356; g) B. Bildstein, M. Malaun, H. Kopacka, K.-H. Ongania, K. Wurst, *J. Organomet. Chem.* **1998**, *552*, 45–61; h) B. Bildstein, M. Malaun, H. Kopacka, K.-H. Ongania, K. Wurst, *J. Organomet. Chem.* **1999**, *572*, 177–187; i) B. Bildstein, M. Malaun, H. Kopacka, K. Wurst, M. Mitterbock, K.-H. Ongania, G. Opromolla, P. Zanello, *Organometallics* **1999**, *18*, 4325–4336; j) C. Bolm, M. Kesselgruber, G. Raabe, *Organometallics* **2002**, *21*, 707–710; k) N. Debono, A. s. Labande, E. Manoury, J.-C. Daran, R. Poli, *Organometallics* **2010**, *29*, 1879–1882; l) S. Gischig, A. Togni, *Organometallics* **2004**, *23*, 2479–2487; m) R. Jackstell, A. Frisch, M. Beller, D. Röttger, M. Malaun, B. Bildstein, *J. Mol. Catal. A* **2002**, *185*, 105–112; n) H. Seo, B. Y. Kim, J. H. Lee, H.-J. Park, S. U. Son, Y. K. Chung, *Organometallics* **2003**, *22*, 4783–4791; o) H. Seo, H.-j. Park, B. Y. Kim, J. H. Lee, S. U. Son, Y. K. Chung, *Organometallics* **2003**, *22*, 618–620; p) U. Siemeling, T. C. Auch, O. Kuhnert, M. Malaun, H. Kopacka, B. Bildstein, *Z. Anorg. Allg. Chem.* **2003**, *629*, 1334–1336; q) U. Siemeling, C. Farber, C. Bruhn, *Chem. Commun.* **2009**, 98–100; r) U. Siemeling, C. Farber, C. Bruhn, M. Leibold, D. Selent, W. Baumann, M. von Hopffgarten, C. Goedecke, G. Frenking, *Chem. Sci.* **2010**, *1*, 697–704; s) D. M. Khramov, E. L. Rosen, V. M. Lynch, C. W. Bielawski, *Angew. Chem.* **2008**, *120*, 2299–2302; *Angew. Chem. Int. Ed.* **2008**, *47*, 2267–2270; t) C. D. Varnado, Jr., V. M. Lynch, C. W. Bielawski, *Dalton Trans.* **2009**, 7253–7261; u) A. Labande, J.-C. Daran, E. Manoury, R. Poli, *Eur. J. Inorg. Chem.* **2007**, 1205–1209; v) E. L. Rosen, C. D. Varnado, A. G. Tennyson, D. M. Khramov, J. W. Kamplain, D. H. Sung, P. T. Cresswell, V. M. Lynch, C. W. Bielawski, *Organometallics* **2009**, *28*, 6695–6706; w) U. Siemeling, C. Färber, M. Leibold, C. Bruhn, P. Mücke, R. F. Winter, B. Sarkar, M. von Hopffgarten, G. Frenking, *Eur. J. Inorg. Chem.* **2009**, 4607–4612.

[14] Plenio previously reported a HG-type catalyst that featured a ferrocene-based NHC phase tag. The oxidation of this complex attenuated RCM activity through precipitation and facilitated catalyst recovery. See: M. Süßner, H. Plenio, *Angew. Chem.* **2005**, *117*, 7045–7048; *Angew. Chem. Int. Ed.* **2005**, *44*, 6885–6888. More recently, Schanz reported that the activities displayed by Grubbs-type olefin metathesis catalysts bearing pH-responsive units were dependent on the degree of protonation. See: S. L. Balof, B. Yu, A. B. Lowe, Y. Ling, Y. Zhang, H.-J. Schanz, *Eur. J. Inorg. Chem.* **2009**, 1717–1722; M. A. Dunbar, S. L. Balof, A. N. Roberts, E. J. Valente, H.-J. Schanz, *Organometallics* **2011**, *30*, 199–203. M. A. Dunbar, S. L.

Balof, L. J. LaBeaud, B. Yu, A. B. Lowe, E. J. Valente, H.-J. Schanz, *Chem. Eur. J.* **2009**, *15*, 12435–12446.

[15] J.-L. Thomas, J. Howarth, K. Hanlon, D. McGuirk, *Tetrahedron Lett.* **2000**, *41*, 413–416.

[16] a) M. C. Jahnke, F. E. Hahn, *Top. Organomet. Chem.* **2010**, *30*, 95–129; b) S. Saravanakumar, M. K. Kindermann, J. Heinicke, M. Kockerling, *Chem. Commun.* **2006**, 640–642.

[17] Free NHC **2** was stable under an inert atmosphere at −35 °C for several days, as determined by ^{1}H NMR spectroscopy (C_6D_6). The NHC was found to decompose over the course of 12 h at 25 °C in C_6D_6.

[18] C. D. Abernethy, J. A. C. Clyburne, A. H. Cowley, R. A. Jones, *J. Am. Chem. Soc.* **1999**, *121*, 2329–2330.

[19] a) D. Chen, V. Banphavichit, J. Reibenspies, K. Burgess, *Organometallics* **2007**, *26*, 855–859; b) W. A. Herrmann, D. Baskakov, E. Herdtweck, S. D. Hoffmann, T. Bunlaksananusorn, F. Rampf, L. Rodefeld, *Organometallics* **2006**, *25*, 2449–2456; c) I. Kownacki, M. Kubicki, K. Szubert, B. Marciniec, *J. Organomet. Chem.* **2008**, *693*, 321–328; d) S. Leuthäußer, D. Schwarz, H. Plenio, *Chem. Eur. J.* **2007**, *13*, 7195–7203; e) M. Viciano, M. Poyatos, M. Sanaú, E. Peris, A. Rossin, G. Ujaque, A. Lledós, *Organometallics* **2006**, *25*, 1120–1134; f) M. Iglesias, D. J. Beetstra, A. Stasch, P. N. Horton, M. B. Hursthouse, S. J. Coles, K. J. Cavell, A. Dervisi, I. A. Fallis, *Organometallics* **2007**, *26*, 4800–4809; g) R. A. Kelly III, H. Clavier, S. Giudice, N. M. Scott, E. D. Stevens, J. Bordner, I. Samardjiev, C. D. Hoff, L. Cavallo, S. P. Nolan, *Organometallics* **2008**, *27*, 202–210.

[20] a) L. Ackermann, A. Fürstner, T. Weskamp, F. J. Kohl, W. A. Herrmann, *Tetrahedron Lett.* **1999**, *40*, 4787–4790; b) M. Scholl, T. M. Trnka, J. P. Morgan, R. H. Grubbs, *Tetrahedron Lett.* **1999**, *40*, 2247–2250; c) T. Weskamp, F. J. Kohl, W. Hieringer, D. Gleich, W. A. Herrmann, *Angew. Chem.* **1999**, *111*, 2573–2576; *Angew. Chem. Int. Ed.* **1999**, *38*, 2416–2419.

[21] a) S. Gessler, S. Randl, S. Blechert, *Tetrahedron Lett.* **2000**, *41*, 9973–9976; b) S. H. Hong, R. H. Grubbs, *J. Am. Chem. Soc.* **2006**, *128*, 3508–3509.

[22] a) S. B. Garber, J. S. Kingsbury, B. L. Gray, A. H. Hoveyda, *J. Am. Chem. Soc.* **2000**, *122*, 8168–8179; b) J. S. Kingsbury, J. P. A. Harrity, P. J. Bonitatebus, A. H. Hoveyda, *J. Am. Chem. Soc.* **1999**, *121*, 791–799.

[23] Compound **6** was obtained via the anion metathesis of **1** with triethyloxonium hexafluorophosphate (see the Supporting Information); see also: P. D. Vu, A. J. Boydston, C. W. Bielawski, *Green Chem.* **2007**, *9*, 1158–1159.

[24] a) J. C. Kotz, C. L. Nivert, J. M. Lieber, R. C. Reed, *J. Organomet. Chem.* **1975**, *91*, 87–95; b) T. M. Miller, K. J. Ahmed, M. S. Wrighton, *Inorg. Chem.* **1989**, *28*, 2347–2355; c) K. Yang, S. G. Bott, M. G. Richmond, *Organometallics* **1995**, *14*, 2387–2394.

[25] G. Altenhoff, R. Goddard, C. W. Lehmann, F. Glorius, *J. Am. Chem. Soc.* **2004**, *126*, 15195–15201.

[26] a) C. A. Tolman, *Chem. Rev.* **1977**, *77*, 313–348. For recent discussions regarding the validity of using TEPs to evaluate the ligand donicities of NHCs, see b) ref. [19g]; c) D. G. Gusev, *Organometallics* **2009**, *28*, 763–770.

[27] A. R. Chianese, X. Li, M. C. Janzen, J. W. Faller, R. H. Crabtree, *Organometallics* **2003**, *22*, 1663–1667.

[28] a) R. Prins, *J. Chem. Soc. D* **1970**, 280b–281; b) T. Sixt, J. Fiedler, W. Kaim, *Inorg. Chem. Commun.* **2000**, *3*, 80–82.

[29] Spectroelectrochemical analysis of $[Ru(PCy_3)Cl_2(=CH\text{-}o\text{-}O\text{-}iPrC_6H_4)]^+$ showed a similar spectrum as $\mathbf{5}^{2+}$ as well as an analogous isobestic point at ~380 nm (see Figure S15 in the Supporting Information); see also: T. Kojima, D. Noguchi, T. Nakayama, Y. Inagaki, Y. Shiota, K. Yoshizawa, K. Ohkubo, S. Fukuzumi, *Inorg. Chem.* **2008**, *47*, 886–895.

[30] a) A. Horsfield, A. Wassermann, *J. Chem. Soc. Dalton Trans.* **1972**, 187–188; b) R. Prins, A. R. Korswagen, *J. Organomet. Chem.* **1970**, *25*, C74–C76; c) R. Prins, F. J. Reinders, *J. Am. Chem. Soc.* **1969**, *91*, 4929–4931.

[31] G. K. Wertheim, R. H. Herber, *J. Chem. Phys.* **1963**, *38*, 2106–2111.

[32] For the performance of other Hoveyda–Grubbs type catalysts under identical conditions, see: T. Ritter, A. Hejl, A. G. Wenzel, T. W. Funk, R. H. Grubbs, *Organometallics* **2006**, *25*, 5740–5745.

[33] For redox switching experiments performed over different timescales, see Figure S17 in the Supporting Information.

[34] Precipitation was not observed during any of the redox cycling events described herein; moreover, no precipitate was collected upon passing any of the oxidized catalysts through 0.2 μm PTFE filters.[14]

[35] As controls, switching experiments were performed using the Hoveyda–Grubbs-type catalyst [Ru(1,3-bis(2,4,6-trimethylphenyl)-2-imidazolylidene)Cl_2(=CH-*o*-O-*i*PrC_6H_4)] (IMes-HG2) under conditions identical to those described above. While IMes-HG2 catalyzed the conversion of **7** ($[\mathbf{7}]_0 = 0.1$ M) to **8** with a $k_{obs} = 2.8 \times 10^{-3}\ s^{-1}$ and the subsequent addition of $[Fe(\eta^5\text{-}C_5H_4COCH_3)Cp][BF_4]$ reduced the measured rate constant ($k_{obs} = 6.8 \times 10^{-5}\ s^{-1}$), catalytic activity spontaneously and steadily increased over time (final $k_{obs} = 4.8 \times 10^{-4}\ s^{-1}$), presumably due to a slow initiation process (see Figure S22 in the Supporting Information). Moreover, the addition of Fc* to the mixture did not significantly alter the measured rate constant ($k_{obs} = 4.0 \times 10^{-4}\ s^{-1}$).

[36] B. Bildstein, A. Hradsky, H. Kopacka, R. Malleier, K.-H. Ongania, *J. Organomet. Chem.* **1997**, *540*, 127–145.

[37] a) F. M. Geisler, G. Helmchen, *J. Org. Chem.* **2006**, *71*, 2486–2492; b) A. Hradsky, B. Bildstein, N. Schuler, H. Schottenberger, P. Jaitner, K.-H. Ongania, K. Wurst, J.-P. Launay, *Organometallics* **1997**, *16*, 392–402.

[38] A. Poater, B. Cosenza, A. Correa, S. Giudice, F. Ragone, V. Scarano, L. Cavallo, *Eur. J. Inorg. Chem.* **2009**, 1759–1766.

[39] J. P. Donahue, *Chem. Rev.* **2006**, *106*, 4747–4783.

[40] a) N. G. Connelly, W. E. Geiger, *Chem. Rev.* **1996**, *96*, 877–910; b) J. R. Aranzaes, M.-C. Daniel, D. Astruc, *Can. J. Chem.* **2006**, *84*, 288–299.

Received: April 2, 2013
Published online: ■■ ■■, 0000

